

In Search of Cyclohexane-like Sn_6^{12-} : Synthesis of $\text{Li}_2\text{Ln}_5\text{Sn}_7$ (Ln = Ce, Pr, Sm, Eu) with an Open-Chain Heptane-like Sn_7^{16-} Instead

Iliya Todorov and Slavi C. Sevov*

Department of Chemistry and Biochemistry, University of Notre Dame, Notre Dame, Indiana 46556

Received December 14, 2006

The title compounds were prepared by direct reactions of the corresponding elements at high temperature. They are isostructural and crystallize in the chiral orthorhombic space group $P2_12_12_1$ ($\text{Li}_2\text{Ce}_5\text{Sn}_7$: $a = 6.273(1)$, $b = 13.839(2)$, and $c = 17.467(2)$ Å; $\text{Li}_2\text{Pr}_5\text{Sn}_7$: $a = 6.241(1)$, $b = 13.762(2)$, and $c = 17.367(1)$ Å; $\text{Li}_2\text{Sm}_5\text{Sn}_7$: $a = 6.262(1)$, $b = 13.809(1)$, and $c = 17.432(1)$ Å; $\text{Li}_2\text{Eu}_5\text{Sn}_7$: $a = 6.165(1)$, $b = 13.562(2)$, and $c = 17.128(1)$ Å). The structure contains isolated Sn_7 oligomers that resemble the carbon core of an open-chain heptane molecule C_7H_{16} . Although these heptamers are stacked along the a axis at a distance that is comparable to the distances within the heptamer, electronic structure calculations show that this intermolecular contact is nonbonding for a formal charge of $16-$ or higher per heptamer. A hypothetical lower charge of $14-$, on the other hand, leads to positive and substantial bond-overlap population that would result in branched infinite chains of $[\text{Sn}_7^{14-}]$. Magnetic measurements of the Ce and Pr compounds indicate a $3+$ oxidation state for the rare-earth cations and, therefore, 17 available electrons from the cations per formula unit. According to four-probe conductivity measurements, the compounds are metallic.

Introduction

Zintl phases are some of the most intriguing and structurally diverse intermetallic compounds (including compounds containing metalloids such as Si, Ge, As, etc.).¹ They combine very electropositive metals such as the alkali, alkaline-earth, and rare-earth elements with less electropositive metals or semimetals such as the heavier post-transition elements. These phases are often described as salts formed upon complete electron transfer from the more to the less electropositive element. Typically, the most interesting feature in such intermetallic compounds is the anionic substructure with its geometry, bonding, and electronic structure. The structural variety of these anionic parts is indeed vast, and often the structures correlate well with the levels of reduction of the corresponding post-transition element. Thus, as more and more electropositive metal is added, the structures change from 3D networks to lower-dimension formations such as layers, chains, clusters, trimers, dimers, and single-atoms, often some of them coexisting together.

One particular system that we and others have studied extensively in the past few years combines alkali metal (A), alkaline-earth (Ae) or lanthanide metal (Ln), and Sn.² Most of the structures in this system are directly related to the average degree of reduction (ADR) of the tin atoms, which can be defined as the average number of negative charges per tin atom, assuming complete electron transfer from the cations. Overall, upon successive reduction, more and more Sn–Sn bonds are broken, and the elemental structure of tin transforms first into clathrate-like 3D structures,³ then into structures with layers and 1D polymers,^{4,5} and finally into

* To whom correspondence should be addressed. E-mail: ssevov@nd.edu.
(1) *Chemistry, Structure, and Bonding of Zintl Phases and Ions*; Kaulzarich, S. M., Ed.; VCH: New York, 1996.

- (2) Reviews: (a) Fässler, T. F.; Hoffmann, S. *Z. Kristallografiya* **1999**, *214*, 722. (b) Pöttgen, R. *Z. Naturforsch., B: Chem. Sci.* **2006**, *61*, 677.
(3) Three-dimensional structures: (a) Dubois, F.; Fässler, T. F. *J. Am. Chem. Soc.* **2005**, *127*, 3264. (b) Fässler, T. F. *Z. Anorg. Allg. Chem.* **2006**, *632*, 1125. (c) Hoffmann, S.; Fässler, T. F. *Inorg. Chem.* **2003**, *42*, 8748. (d) Bobev, S.; Sevov, S. C. *J. Am. Chem. Soc.* **2001**, *123*, 3389. (e) Fässler, T. F.; Kronseder, C. *Angew. Chem., Int. Ed.* **1998**, *37*, 124. (f) Fässler, T. F.; Kronseder, C. *Z. Anorg. Allg. Chem.* **1998**, *624*, 561. (g) Vaughey, J. T.; Corbett, J. D. *Inorg. Chem.* **1997**, *36*, 4316. (h) Zhao, J. T.; Corbett, J. D. *Inorg. Chem.* **1994**, *33*, 5721.
(4) Two-dimensional structures: (a) Dubois, F.; Schreyer, M.; Fässler, T. F. *Inorg. Chem.* **2005**, *44*, 477. (b) Fässler, T. F.; Hoffmann, S. *Inorg. Chem.* **2003**, *42*, 5474. (c) Fässler, T. F.; Hoffmann, S.; Kronseder, C. *Z. Anorg. Allg. Chem.* **2001**, *627*, 2486. (d) Bobev, S.; Sevov, S. C. *Inorg. Chem.* **2000**, *39*, 5930.

structures with isolated clusters.^{6–17} For example, tin structures with an ADR of less than -0.4 per tin atom such as $\text{Na}_5\text{Sn}_{13}$ ($\text{ADR} = -5/13 = -0.38$),^{3g} $\text{K}_{8-x}\text{Sn}_{25}$ (≤ -0.32),^{3h} and NaSn_5 (-0.20) are 3D frameworks.^{3e} The more-reduced compounds $\text{Na}_7\text{Sn}_{12}$ (-0.58) and $\text{A}_3\text{Na}_{10}\text{Sn}_{23}$ (-0.56 ; $\text{A} = \text{K}, \text{Rb}, \text{Cs}$),^{4b,4d} on the other hand, exhibit layered structures. Further reduction results, for example, in the recently characterized Na_4CaSn_6 (-1.00) with isolated 1D cylindrical tubes of interconnected cyclohexane-like Sn_6^{6-} units with three-bonded tin atoms that are formally Sn^- .^{5b} This trend would suggest that zero-dimensional species should appear at even greater reduction levels. However, electron-poor clusters, analogous to the cage-like boranes, appear at less-negative ADRs. For example, *nido*- Sn_9^{4-} and *arachno*- Sn_8^{6-} are found in $\text{A}_{12}\text{Sn}_{17}$ (-0.7) and $\text{A}_4\text{Li}_2\text{Sn}_8$ (-0.75), respectively.^{8,14} Bonding in these species is achieved via delocalized electrons that are fewer than those needed for normal two-center–two-electron bonds for the Sn–Sn contacts, a phenomenon that is often referred to as σ or 3D delocalization. Clusters with normal two-center–two-electron bonds are also known, and their charges depend on the number of bonds per tin atom. For example, both tetrahedra and truncated tetrahedra are known for tin. They are made of three-bonded vertices, that is, Sn^- , and their charges match the numbers of atoms in the cluster, that is, Sn_4^{4-} and Sn_{12}^{12-} observed in A_4Sn_4 (-1.00) and $\text{AeNa}_{10}\text{Sn}_{12}$ (-1.00), respectively.^{11,17}

An average degree of reduction beyond -1.00 can be handled either by increasing the number of two-, one-, and zero-bonded tin atoms or by adding π -delocalization on top of a formally localized σ -bonded manifold. The latter has been achieved in a series of compounds with discrete aromatic pentagonal rings of Sn_5^{6-} analogous to the cyclopentadienyl anion C_5H_5^- as well as in compounds with flat zigzag chains with a conjugated π -system analogous to the polyacetylenes. Examples are Na_8BaSn_6 (-1.67),⁶ Na_8EuSn_6 (-1.67),⁶ $\text{Li}_{9-x}\text{CaSn}_{6+x}$ (~ -1.69),⁷ $\text{Li}_{9-x}\text{EuSn}_{6+x}$ (~ -1.69),⁷ $\text{Li}_5\text{Ca}_7\text{Sn}_{11}$ (-1.73),⁷ and $\text{Li}_6\text{Eu}_5\text{Sn}_9$ (-1.78) with Sn_5^{6-} .⁷ $\text{Li}_6\text{Eu}_5\text{Sn}_9$ and the most-reduced $\text{LiMgSr}_2\text{Sn}_3$ (-2.33) and $\text{LiMgEu}_2\text{Sn}_3$ (-2.33) contain infinite and flat zigzag chains of tin.⁷ The existence of cyclopentadienyl-like Sn_5^{6-} led to an attempted synthesis of benzene-like Sn_6^{6-} in the compound Na_4CaSn_6 . However, although a compound with this exact stoichiometry was synthesized, its structure

revealed that it contains tubes of stacked and interconnected cyclohexane-like Sn_6^{6-} units instead.^{5b} All of the tin atoms in the tubes are three-bonded, thus the charge of $6-$ per Sn_6 repeating unit. The existence of these interconnected cyclohexane-like formations, in turn, suggested the possible existence of their isolated analogs. Thus, our next step was to attempt the synthesis of isolated cyclohexane-like species made of six two-bonded tin atoms, that is, Sn_6^{12-} . These attempts led to the synthesis and structural characterization reported here of four isostructural compounds $\text{Li}_2\text{Ln}_5\text{Sn}_7$ ($\text{Ln} = \text{Ce}, \text{Pr}, \text{Sm}, \text{Eu}$) that contain isolated heptane-like Sn_7^{16-} instead. The open-chain heptamers are made of five two-bonded and two one-bonded tin atoms and exemplify the notion that high levels of reduction (ADR of -2.43) can be handled by lowering the number of bonds to the tin atoms even further.

Experimental Section

Synthesis. All of the manipulations were performed in an argon-filled glovebox (moisture level below 0.1 pm). The starting materials Li (granular, Acros, 99+%), Ce (ingot, Alfa, 99.9%), Pr (ingot, Ames Laboratory DOE, 99.9%), Sm (ingot, Ames Laboratory DOE, 99.9%), Eu (ingot, Ames Laboratory DOE, 99.9%), and Sn (rod, Alfa, 99.999%) were used as received. In a typical reaction, the elements were placed in a niobium ampule that was then sealed by arc-welding under argon. This container was, in turn, sealed in a fused-silica tube under vacuum. Initially, $\text{Li}_2\text{Eu}_5\text{Sn}_7$ was found as a minor phase in the product from a reaction with nominal composition $\text{Li}_6\text{Eu}_3\text{Sn}_6$ in an attempt to synthesize isolated cyclohexane-like Sn_6^{12-} . The mixture was heated at 800 °C for 2 days and cooled down by turning off the furnace. The other products of this reaction were the known $\text{Li}_6\text{Eu}_5\text{Sn}_9$ and traces of $\text{Li}_{9-x}\text{EuSn}_{6+x}$.⁷ After the stoichiometry of the new compound was determined to be $\text{Li}_2\text{Eu}_5\text{Sn}_7$ from single-crystal X-ray diffraction, various reactions with different lanthanides were carried out at different temperatures. Isostructural compounds were obtained for Ce, Pr, and Sm, whereas reactions with La, Nd, Gd, Dy, and Yb produced other compounds. $\text{Li}_2\text{Eu}_5\text{Sn}_7$ and $\text{Li}_2\text{Sm}_5\text{Sn}_7$ could not be prepared as single phases. The Ce and Pr analogs, however, were obtained pure by using a slight excess of Li and heating the samples at 860 °C for 2 weeks, followed by cooling down at a rate of 1 °C/min.

Structure Determination. Silver-gray bar-like crystals with metallic luster were selected from each compound and were mounted in thin-walled glass capillaries that were subsequently flame-sealed at both ends. The crystals were checked for singularity by X-ray diffraction using an Enraf-Nonius CAD4 diffractometer with graphite monochromated $\text{Mo K}\alpha$ radiation ($\lambda = 0.71073$ Å). Room-temperature data were collected from a crystal of $\text{Li}_2\text{Ce}_5\text{Sn}_7$ ($0.2 \times 0.12 \times 0.08$ mm³). The raw data (a quadrant of a sphere, $\omega - 2\theta$ scans, $\theta_{\text{max}} = 25^\circ$) were corrected for absorption with the aid of the average of three ψ scans. The observed extinction conditions and the intensity statistics suggested only the non-centrosymmetric space group $\text{P}2_12_1$ ($a = 6.273(1)$, $b = 13.839(2)$, and $c = 17.467(2)$ Å). The structure was solved and refined on F^2 in that space group with the aid of the SHELXTL-V5.1 software package.¹⁸ Direct methods provided the positions of the Ce and Sn atoms, whereas the Li cations were later located from difference Fourier maps and were refined only isotropically. Details of the data collection and structure refinement are given in Table 1. The

(5) One-dimensional structures: (a) Bobev, S.; Sevov, S. C. *J. Alloys Compd.* **2002**, *338*, 87. (b) Todorov, I.; Sevov, S. C. *Inorg. Chem.* **2006**, *45*, 4478.

(6) Todorov, I.; Sevov, S. C. *Inorg. Chem.* **2005**, *44*, 5361.

(7) Todorov, I.; Sevov, S. C. *Inorg. Chem.* **2004**, *43*, 6490.

(8) Hoch, C.; Wendorff, M.; Rohr, C. *J. Alloys Compd.* **2003**, *361*, 206.

(9) Bobev, S.; Sevov, S. C. *J. Am. Chem. Soc.* **2002**, *124*, 3359.

(10) Hoch, C.; Wendorff, M.; Rohr, C. *Acta Crystallogr., Sect. C: Cryst. Struct. Commun.* **2002**, *58*, 145.

(11) Bobev, S.; Sevov, S. C. *Inorg. Chem.* **2001**, *40*, 5361.

(12) Zurcher, F.; Nesper, R.; Hoffmann, S.; Fässler, T. F. *Z. Anorg. Allg. Chem.* **2001**, *627*, 22211.

(13) Klem, M. T.; Vaughney, J. T.; Harp, J. G.; Corbett, J. D. *Inorg. Chem.* **2001**, *40*, 7020.

(14) Bobev, S.; Sevov, S. C. *Angew. Chem., Int. Ed.* **2000**, *39*, 4108.

(15) Leon-Escamilla, E. A.; Corbett, J. D. *Inorg. Chem.* **1999**, *38*, 738.

(16) Ganguli, A. K.; Guloy, A. M.; Leon-Escamilla, E. A.; Corbett, J. D. *Inorg. Chem.* **1993**, *32*, 4349.

(17) Grin, Y.; Baitinger, M.; Kniep, R.; von Schnering, H. G. *Z. Kristallografia* **1999**, *214*, 415.

(18) SHELXTL, version 5.1; Bruker Analytical Systems: Madison, WI, 1997.

Table 1. Selected Data Collection and Refinement Parameters for $\text{Li}_2\text{Ce}_5\text{Sn}_7$

chemical formula	$\text{Li}_2\text{Ce}_5\text{Sn}_7$
fw	1545.31
No.	$P2_12_12_1$, 4
a (Å)	6.2772(7)
b (Å)	13.8384(9)
c (Å)	17.4663(9)
V (Å ³)	1517.2(2)
$\lambda(\text{Mo K}\alpha)$ (Å)	0.710 73
ρ_{calcd} (g·cm ⁻³)	6.765
μ (cm ⁻¹)	25.909
R1/wR2, ^a I \geq 2 σ _I (%)	2.76/6.71
R1/wR2, ^a all data(%)	2.89/6.76

^a R1 = $[\sum||F_o| - |F_c||]/\sum|F_o|$; wR2 = $\{[\sum w[(F_o)^2 - (F_c)^2]^2]/\sum w(F_o)^2\}^{1/2}$; $w = [\sigma^2(F_o)^2 + (0.034P)^2 + 0.1256P]^{-1}$ where $P = [(F_o)^2 + 2(F_c)^2]/3$.

single crystals of isostructural $\text{Li}_2\text{Sm}_5\text{Sn}_7$, $\text{Li}_2\text{Pr}_5\text{Sn}_7$, and $\text{Li}_2\text{Eu}_5\text{Sn}_7$ were of unsatisfactory quality for data collection; therefore, only lattice parameters were determined for these compounds ($\text{Li}_2\text{Pr}_5\text{Sn}_7$: $a = 6.241(1)$, $b = 13.762(2)$, and $c = 17.367(1)$ Å; $\text{Li}_2\text{Sm}_5\text{Sn}_7$: $a = 6.262(1)$, $b = 13.809(1)$, and $c = 17.432(1)$ Å; $\text{Li}_2\text{Eu}_5\text{Sn}_7$: $a = 6.165(1)$, $b = 13.562(2)$, and $c = 17.128(1)$ Å).

Property Measurements. The magnetizations of 15.5 mg of $\text{Li}_2\text{Ce}_5\text{Sn}_7$ and 56.3 mg of $\text{Li}_2\text{Pr}_5\text{Sn}_7$ were measured in the temperature range of 10–250 K and under a field of 3 T on a Quantum Design MPMS SQUID magnetometer. The samples were sealed in quartz tubes between pairs of quartz rods that fit tightly in the tubes. The data were corrected for the holder and for ion-core diamagnetism. The room-temperature electrical resistivities of $\text{Li}_2\text{Ce}_5\text{Sn}_7$ and $\text{Li}_2\text{Pr}_5\text{Sn}_7$ were measured by the four-probe method (an in-line probe from Jandel) on pressed pellets (2000–3000 psi, 1.6 mm thick). Measured was the drop of voltage across the samples at constant currents.

Electronic Structure Calculations. Extended Hückel calculations were carried out within the tight-binding approximation with only the tin atoms included (H_{ii} and ζ_1 for Sn 5s: -16.16 eV and 2.12, for Sn 5p: -8.32 eV and 1.82).¹⁹ A molecular orbital diagram was calculated for the isolated heptamer as well as for a dimer of heptamers positioned with respect to each other exactly as in the structure. Density of states (DOS) and crystal orbital overlap population (COOP) curves were calculated for the whole tin substructure (240 k-points).

Results and Discussion

Structure. The structure of the isostructural title compounds is very simple and easy to visualize (Figure 1). It is made of isolated seven-atom oligomers of tin, Sn_7 , and lithium and rare-earth cations that separate and screen the negative charges of the oligomers with $d(\text{Li}-\text{Sn}) \geq 2.72$ Å, $d(\text{Ce}-\text{Sn}) \geq 3.18$ Å, $d(\text{Ce}-\text{Li}) \geq 3.40$ Å, and $d(\text{Ce}-\text{Ce}) \geq 3.94$ Å. It should be mentioned that the full occupancy of the lithium sites cannot be guaranteed by X-ray diffraction. However, in light of the large size of the coordination spheres around the lithium atoms, it is very unlikely that there could be such large empty holes in the structure. The tin heptamers are puckered in all three directions and resemble an open-chain, normal heptane, $n\text{-C}_7\text{H}_{16}$ (Figure 2). The distances and angles within the oligomers range from 2.930 Å and from 86.63 to 150.98°, respectively. These distances are

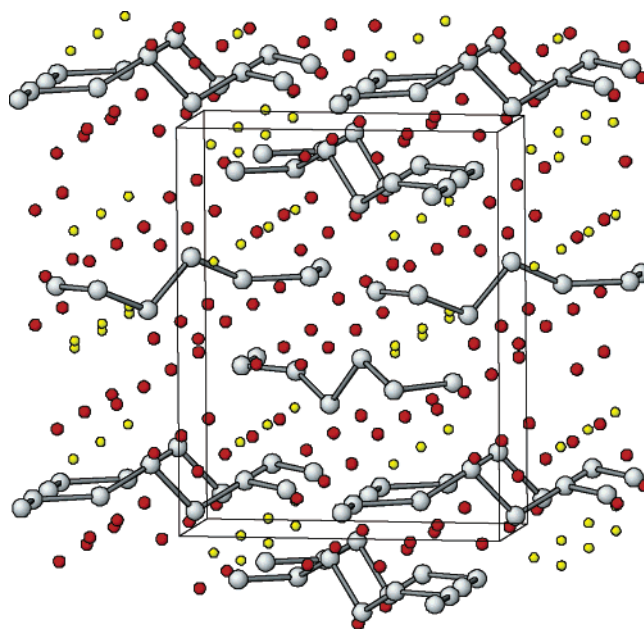


Figure 1. View of the structure of $\text{Li}_2\text{Ln}_5\text{Sn}_7$ (Ln = Ce, Pr, Sm, Eu) along the a axis of the orthorhombic cell (b is horizontal). Isolated seven-atom tin oligomers, Sn_7 , are embedded in a matrix of lithium (yellow) and rare-earth (red) cations.

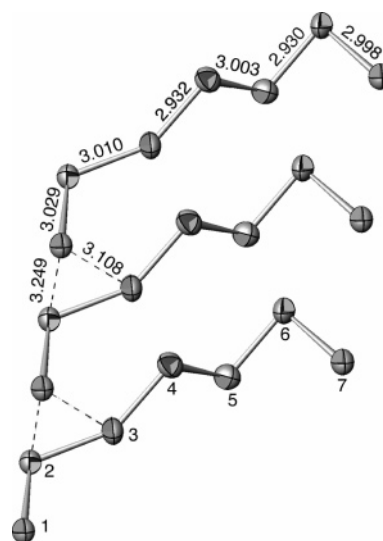


Figure 2. Close view of the tin heptamers stacked along a . Some important angles (deg): Sn1–Sn2–Sn3, 117.97(3); Sn4–Sn3–Sn2, 150.98(3); Sn5–Sn4–Sn3, 111.50(3); Sn6–Sn5–Sn4, 113.11(3); Sn7–Sn6–Sn5, 86.63(3); Sn1...Sn3–Sn2, 59.40(2). (All of the distances and angles are for $\text{Li}_2\text{Ce}_5\text{Sn}_7$.)

quite typical for single Sn–Sn bond distances, whereas the angles at Sn2, Sn4, and Sn5 are typical for sp^3 hybridized atoms (Figure 2). The angles at Sn3 and Sn6, however, deviate significantly from tetrahedral, and the reasons for this are found in the electronic structure of the compound (below). The oligomers are well separated along b and c but have one very close contact of 3.108 Å along a as shown in Figure 2. The cations wrap around the oligomer with six to eight cations around each tin atom.

Electronic Structure. Complete electron transfer from the cations to the tin heptamers results in a formal charge of 17⁻ per heptamer, that is, Sn_7^{17-} . (Cerium in the structure is Ce^{3+} according to the magnetic measurements and the

(19) (a) Hoffmann, R. *J. Chem. Phys.* **1963**, 39, 1397. (b) Whangbo, M.-H.; Hoffmann, R. *J. Am. Chem. Soc.* **1978**, 100, 6093.

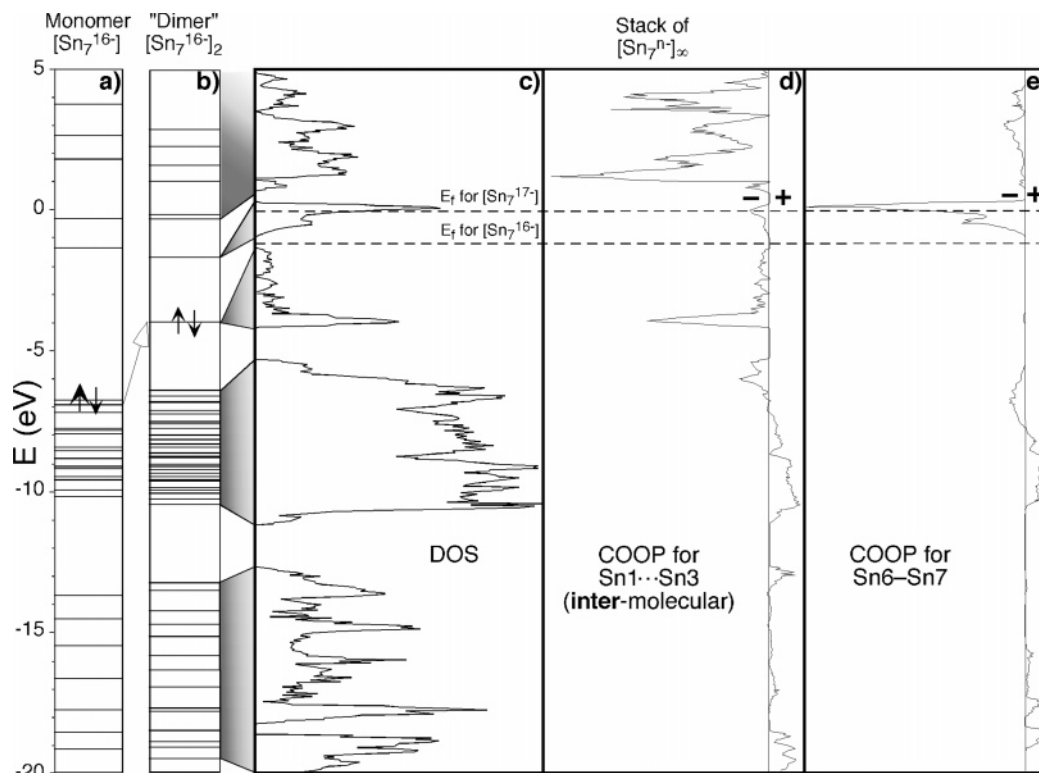


Figure 3. Results from extended Hückel calculations performed on (a) an isolated heptamer, (b) a dimer of heptamers positioned as in the structure (Figure 2), (c–e) the observed infinite stack of heptamers. Shown in (a–c) is how the MO diagram expands into DOS bands. The COOP curves for the Sn1–Sn3 and Sn6–Sn7 contacts are shown in d and e, respectively.

existence of the isostructural compounds with Pr, Sm, and Eu.) The molecular orbital diagrams for the isolated heptamer shows, as expected, a sizable HOMO–LUMO gap for the charge of 16^- , that is, for Sn_7^{16-} (Figure 3a). After all, the 16 additional electrons correspond to the 16 hydrogen atoms in the analogous neutral hydrocarbon heptane, C_7H_{16} . The analogy can be extended even further by realizing that the 16 C–H bonds in the latter correspond to 16 lone pairs of electrons on the tin atoms. Thus, the two terminal tin atoms, Sn1 and Sn7, have three such lone pairs each, whereas each of the remaining five atoms has two lone pairs. The total of 44 required electrons for 6 bonds and 16 lone pairs are available from the 7 Sn atoms providing 4 electrons each and the 16 additional electrons from the charge.

Bringing two heptamers close to each other as in the structure leads to interactions between the lone-pair orbitals of the contact atoms. There is one such contact per two heptamers and it occurs between atoms Sn1 and Sn3 at a distance of 3.108 Å (Figure 2). The geometry at the contact allows for direct head-to-head interactions between one of the three lone-pair orbitals at the terminal Sn1 with one of the two lone-pair orbitals of the two-bonded Sn3. This leads to one bonding and one more-strongly antibonding combinations that are both occupied for the charge of 16^- per heptamer (the antibonding MO is at -4 eV in Figure 3b). Therefore, the overall interaction between the two heptamers is antibonding, and although the inter-heptamer distance is only 3.108 Å, there is no bond between the two heptamers for this electron count. However, there would be a bond for an electron count that is lower by one per heptamer, that is, for Sn_7^{15-} , and will result in a 14-atom molecule Sn_{14}^{30-}

with a good HOMO–LUMO gap (the MO at -4 eV in Figure 3b would be empty and become the LUMO). This essentially means that two lone pairs of electrons would be replaced with one bonding pair of electrons for such a hypothetical species. Lastly, there are no inter-heptamer interactions between Sn1···Sn2 despite the distance of 3.249 Å. The lack of interactions in this case is not so much based on the distance as on the angles at the corresponding atoms. Thus, the angles Sn1···Sn2–Sn3 and Sn2···Sn1···Sn3 are 59.4 and 56.5°, respectively, and, furthermore, Sn1···Sn2 is collinear with Sn1–Sn2 adjacent to it (Figure 2).

The above analysis for a dimer of heptamers can be extended to an infinite stack of heptamers by recognizing that each heptamer has two short contacts with its two neighbors as shown for the middle heptamer in Figure 2. Therefore, if these contacts are to become bonds, each heptamer needs to reduce its charge by two. Thus, a stack of Sn_7^{14-} would be an all-bonded infinite chain of $\{-(\text{Sn}_7^{14-})-\}_\infty$. This is clearly seen in the density of states (DOS) calculated for the stack of heptamers shown in Figure 3c. The band generated by the bonding molecular orbitals within the heptamer (made predominantly of tin *p* states) spans from -11.2 to -5.2 eV. It is separated by a band gap of about 1.1 eV from the band that develops from the inter-heptamer Sn1···Sn3 antibonding interactions (-4.1 to -1.2 eV). However, for a heptamer with a charge of 16^- or more, this latter band is filled and cancels out any bonding between the heptamers. This is clearly seen from the COOP curve calculated for the inter-heptamer contact of 3.108 Å between Sn1 and Sn3 (Figure 3d) which shows that the -4.1 to -1.2 eV band arises exclusively from the Sn1···Sn3 antibonding

interactions. Even more indicative of these interactions is the bond overlap population (BOP) for this contact calculated for charges of 14⁻ and 16⁻, 0.33 and 0.08, respectively. In comparison, the bond overlap populations for the bonds within the heptamer for a charge of 14⁻ are within the range of 0.35–0.47 and change only very slightly on going to a charge of 16⁻, from 0.20 to 0.45. Also in comparison, the BOP for the longer inter-heptamer contact of 3.249 Å is zero even for a charge of 14⁻ and becomes very negative, -0.27 for the charge of 16⁻. This confirms that this contact is definitely nonbonding to antibonding.

Had the number of available extra electrons (from the counteranions) per heptamer been 16, the resulting compound would have been electronically balanced with a small band gap (calculated at ca. 0.3 eV). However, the formula Li₂Ce₅Sn₇ provides 17 extra electrons per heptamer. The additional electron partially fills a conduction band that is above the small-band gap (Figure 3c). This band is also somewhat separated from the rest of the antibonding states above it. Studies of the COOP curves for all of the Sn–Sn contacts and the corresponding BOPs revealed that this band corresponds solely to the Sn6–Sn7 interactions in the heptamer and is antibonding (Figure 3d). Thus, the Sn6–Sn7 BOP for charges of 14⁻, 16⁻, and 17⁻ is 0.41, 0.40, and -0.01, respectively, whereas the BOPs for the rest of the interactions within the heptamer remain essentially unchanged. The Sn6–Sn7 antibonding band can carry two electrons, and at a charge of 17⁻ it is exactly half-filled. A completely filled band would result in a charge of 18⁻ per seven tin atoms and would result in the complete separation of the Sn7 atom from the rest of the oligomer. It would result in a hexamer with a charge of 14⁻, that is, Sn₆¹⁴⁻, and an isolated tin atom with a charge of 4⁻, that is, Sn⁴⁻. The half-filled band is either the cause for or the result of the very substantial deviation of the angle at Sn6, 86.63°, from a tetrahedral angle. At the same time, the Sn6–Sn7 distance does not differ from the rest of the Sn–Sn distances within the heptamer. It is primarily the angular positioning of Sn7 with respect to the Sn5–Sn6 bond that is very different from the rest of the heptamer. Of course, the extra electron is not localized only on the tin heptamer but is, rather, delocalized over the structure including lithium- and cerium-generated bands that overlap with the Sn6–Sn7 antibonding band. This provides the observed metallic properties of the compound.

Properties. The measured room-temperature resistivities of 5.8×10^{-6} and $5.6 \times 10^{-6} \Omega \cdot \text{cm}$ for Li₂Ce₅Sn₇ and Li₂Pr₅Sn₇, respectively, confirm the metallic properties of the compounds predicted from the electronic structure calculations. These values are only an order of magnitude higher than the resistivity of elemental tin, $9.17 \times 10^{-7} \Omega \cdot \text{cm}$, and indicate that the compounds are fairly good conductors.

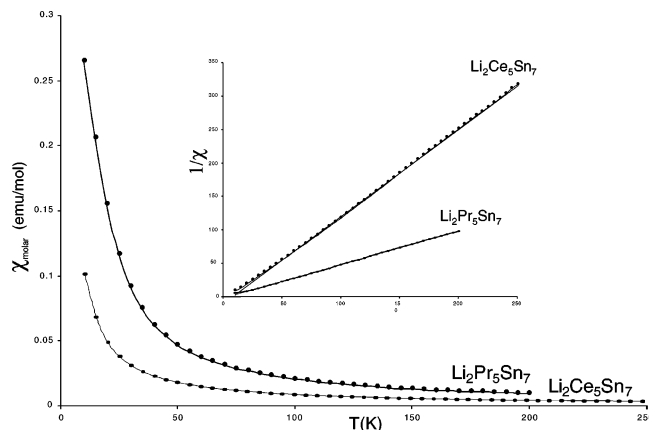


Figure 4. Plots of the molar susceptibilities of Li₂Ce₅Sn₇ and Li₂Pr₅Sn₇ as functions of the temperature. The inset shows linear fits of $1/\chi(T)$ for the two compounds.

As expected, Li₂Ce₅Sn₇ and Li₂Pr₅Sn₇ are paramagnetic with Curie–Weiss temperature dependence of the magnetic susceptibility (Figure 4). Fitting the $1/\chi(T)$ plots with straight lines yielded effective magnetic moments of $\mu_{\text{eff}} = 2.50\mu_{\text{B}}$ and $3.94\mu_{\text{B}}$ per Ce and Pr atom, respectively. These values are very close to the expected moments for Ce³⁺ and Pr³⁺, $2.54\mu_{\text{B}}$ and $3.58\mu_{\text{B}}$, respectively.²⁰

Conclusions

The new ternary zintl compounds Li₂Ln₅Sn₇ (Ln = Ce, Pr, Sm, Eu) contain isolated heptane-like Sn₇ oligomers that are stacked at close distance to each other. They would have been interconnected into an infinite chain had there been only 14 electrons provided by the counteranions in an imaginary compound, Li₂Ln₄Sn₇. However, 16 of the available 17 electrons (2 from Li and 3×5 from Ln) fill all of the antibonding states of the inter-heptamer interactions and result in isolated species. The 17th electron partially occupies an antibonding band that corresponds to the Sn–Sn bond of a terminal tin atom. It is delocalized over this band and empty alkali-metal and lanthanide *s* states and makes the compounds metallic.

Acknowledgment. We thank the National Science Foundation for the financial support of this research (grant no. CHE-0446131).

Supporting Information Available: X-ray crystallographic file. This material is available free of charge via the Internet at <http://pubs.acs.org>.

IC062390H

(20) Kittel, C. *Introduction to Solid State Physics*, 2nd ed.; Wiley: New York, 1956; p 218.